Quantum sensing with a hybrid silicon nitride / diamond photonics platform

N. Verellen,[1,2] B. Van de Vel,[1,2] S. Philips,[1,2] F. James Shirley,[1,2] T. Hantschel,[2] and P. Van Dorpe[1,2]

[1] KU Leuven, Dept. of Physics and Astronomy, Celestijnenlaan 200D, B-3001 Leuven, Belgium
[2] imec, Kapeldreef 75, B-3001 Leuven, Belgium

Diamond nitrogen vacancy (NV) centers extend the frontiers of detection and imaging techniques beyond classical limits. This unique quantum sensor can be optically initialized and read out by means of optically detected magnetic spin resonance (ODMR). Large-scale and cost-effective integration in diamond is hampered by the lack of chip-scale high-quality substrates. We experimentally demonstrate the integration of NV centers into a silicon nitride photonic circuit and provide the first ODMR magnetic field sensing using a mature technology platform. Nano-analytic applications range from life sciences to material science. Being a solid-state qubit, establishing a platform to interface with NV centers is essential for the development of quantum information technologies.

Introduction

The nitrogen vacancy (NV) center is a paramagnetic and photoluminescent point defect in the diamond carbon lattice. It has become a promising candidate for real-space nanometer-scale ultra-sensitive probing of magnetic fields, electrical currents, temperature, and even single electron and nuclear spins—all under ambient conditions [1]. The sensing principle is based on the optical detection of the electron spin state of the NV centers and is known as optically detected magnetic resonance (ODMR). A simplified electronic structure of the NV center is shown in Figure 1a. The NV center spin can optically be polarized in the $m_s = 0$ state which corresponds to maximum photoluminescence (PL). The spin can also be manipulated by microwaves (MW) inducing resonant transitions between the $m_s = 0$ and $m_s = \pm 1$ states (electron spin resonance (ESR)), which is accompanied by a drop in the PL intensity. NV centers can be introduced by ion beam implantation or doping during CVD growth in diamond crystals and in diamond nanoparticles, known as nanodiamonds (NDs). The properties of this solid-state system engage a whole new paradigm in metrology and sensing. The nano-analytic applications range from life sciences to material science and technology. The diamond NV center is also well-known as a solid-state qubit, rendering it one of the leading candidates for quantum information technologies. The establishment of a technology platform to interface with these centers is essential for further developments. However, large-scale and cost-effective integration in diamond is hampered by the lack of chip-scale high-quality substrates and challenges of large-scale patterning. Silicon nitride (Si_3N_4) photonics, on the other hand, is a mature platform that is compatible with CMOS-based processing, making it possible to fabricate complex, large-scale and low-cost integrated photonic circuits. Moreover, its transparency window matches perfectly with the visible excitation and emission wavelengths of diamond NV centers. Recently, a silicon nitride photonic

circuit with integrated long-lived quantum memories based on NV centers in diamond micro waveguides was demonstrated [2].
Here, we experimentally demonstrate that the evanescent tail of a SiN waveguide mode can optically polarise the NV center spin states in NDs and that the spin state can remotely be detected by coupling the PL light back into the waveguide. To illustrate this quantum metrology functionality, an ODMR magnetic field sensing experiment is performed.

Methods

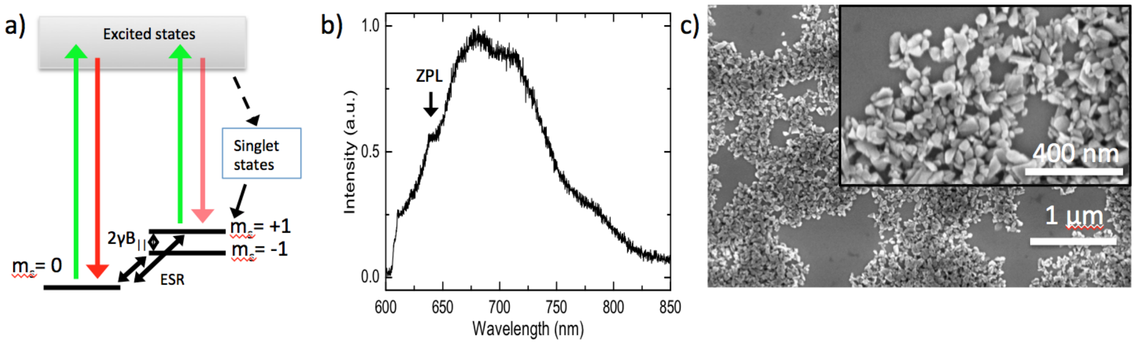

Figure 1: a) Electronic energy level structure of the diamond NV^- center. By applying resonant microwaves, the spin state is manipulated by exiting electron spin resonance (ESR) transitions. b) Emission spectrum of the diamond nanoparticles excited by a 532 nm CW laser. A zero phonon line at 637 nm is observed, accompanied by a broad phonon sideband. Integration time 10 s. c) SEM images of the dropcasted NDs.

The Si_3N_4 components were fabricated on a quartz substrate using a low temperature plasma-enhanced CVD process optimized to achieve the lowest material autofluorescence—crucial for the detection of low intensity fluorescence signals [3, 4]. The Si_3N_4 layer is 180 nm thick. The width of the waveguides is choosen as to result in single mode propagation for the emission of the NV center. A top cladding of 2 μm SiO_2 on top of the chip reduces propagation losses in the waveguides. This cladding layer is locally removed to create an open-clad region where the NDs are deposited. NDs supended in water with a concentration of 1mg/mL are dropcasted in the open-clad region and let to dry in open air. The NDs have a diameter of ∼35 nm and are strongly doped with NV centers (>15 per particle). The emission spectrum is shown in Figure 1b and a scanning electron microscopy (SEM) image of the particles dropcasted on a Si substrate is shown in panel c. MWs are sent to the NDs by means of a coplanar waveguide underneath the sample. For optical excitation of the NV centers, a continuous wave laser at 532 nm is used. Collection of the emission is done by an NA=0.95, 100X magnification objective and detected by a single-photon counting module after passing through a 620 nm long pass filter.

Results

To demonstrate the coupling of the diamond nanoparticles to the SiN photonics system, we performed two sets of experiments as illustrated in Figure 2a and b. In the first configuration (panel a), the NDs in the open-clad region are excited by the evanescent field tail of the SiN waveguide. Light is coupled into this waveguide by a grating coupler 16

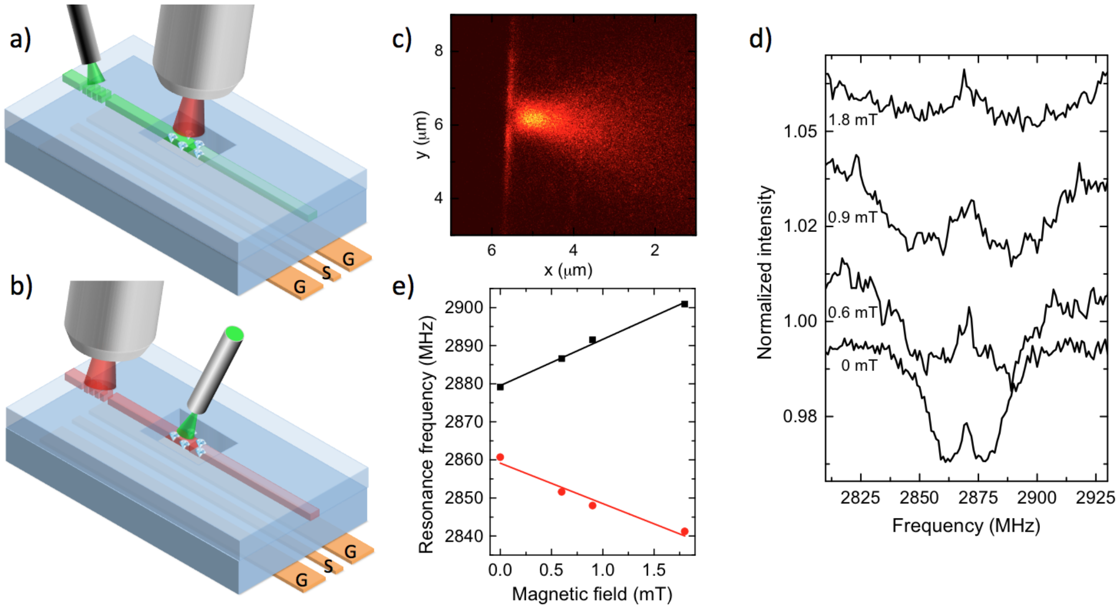

Figure 2: Diamond ODMR with SiN photonics. a) Evanescent waveguide field excitation of NDs dropcasted in an open-clad region. 532 nm laser light from an optical fiber is coupled into the waveguide by a grating. MW manipulation of the NV electron spins is enabled by a coplanar waveguide underneath the chip (S = signal; G = ground). b) Reversed configuration with direct excitation at the open-clad and detection at the grating. c) Confocal scan of the NV emission on top of the waveguide when entering the open-clad region. d) ODMR spectra with increasing external magnetic field. Laser power of 160 μW at the fiber, MW power of 3 W, detector integration time of 100 ms and averaging of 20 frequency sweeps was used. e) Resonance frequencies fitted from panel d versus applied field. Full lines are linear fits indicating the expected linear Zeeman shift.

mm away from the NDs. Simulations indicate an excitation efficiency by the evanescent field of the waveguide on the order of 1%. The emission is collected confocally by the objective. An XY-scan at the edge of the open-clad region (cladding on the left, ND on the right) is shown in panel c. The maximum intensity is situated close to the edge after which it decreases exponentially due to the strong scattering of the excitation light by high concentration of ND scatterers. After verifying the emission spectrum (Figure 1), an ODMR spectrum is taken as shown in 2d (bottom curve). Due to lattice strain in the particles, a splitting in resonance frequencies of the $m_s = \pm 1$ states is observed. The signal contrast ($1 - PL_{\text{on res}}/PL_{\text{off res}}$) is 2.7%. We then applied a magnetic field by approaching a permanent magnet to the sample. The field strength in function of distance from the magnet was determined using a Gauss meter. When a magnetic field is applied, a Zeeman split of the degenerate $m_s = \pm 1$ electron spin states occurs with a magnitude of $2\gamma B_{||}$. Here is γ the gyromagnetic ratio and $B_{||}$ the component of the magnetic field parallel to the orientation of the NV center. The resulting ODMR spectra in panel d show a clear splitting of the resonances and spectral broadening. This broading is the result of the random orientation of the ND particles, and hence random field projection $B_{||}$. In panel e the electron spin resonance frequencies are plotted in function of the applied external field. The linear fits through these data points (full lines) verify the expected linear

dependence and reveal a spectral shift of 11 MHz/mT.
The same set of measurements is performed for the second configuration illustrated in Figure 2b where now the NV centers are excited directly at the open-clad region by the green laser through the optical fiber. The emission is collected through near-field coupling into the waveguide and coupled out at a remote (16 mm) output grating. Simulations indicate a collection efficiency on the order of 4% for NDs placed on top of the waveguide. A linear shift of the ODMR frequencies of 10 MHz/mT is obtained.
An expression for the sensitivity of the magnetic field sensor is given by [1]:
$\eta = \frac{4h\,FWHM}{3\sqrt{3}g\mu_B C\sqrt{n}}$ with g the Landé constant, μ_B the Bohr magneton, C the contrast and n the photon counts (in Hz) at resonance. This leads to values of respectively 27 μT/$\sqrt{\text{Hz}}$ and 23 μT/$\sqrt{\text{Hz}}$ for evanescent field excitation and near-field collection configurations. In our experiments n was on the order of 40 kcounts/s for a laser power of 160 μW at the fiber. The ODMR resonance line width (FWHM) was 17 MHz for B_{ext} = 0.

Conclusions

We have demonstrated magnetic field sensing by optically detecting the electron spin state of nitrogen vacancy centers in diamond nanoparticles using a simple SiN integrated photonic circuit. We performed this ODMR measurements in two configurations: 1) the evanescent tail of the SiN waveguide mode excites the NV centers and the PL signal is detected directly; 2) the NV centers are excited at an open clad region and the near-field emission is coupled into the waveguide and remotely detected at an output grating. These constitute the first steps towards a hybrid platform for integrated photonics quantum metrology. The obtained sensitivity values of 25 μT/$\sqrt{Hz}$ are of the same order as those recently demonstrated for remote sensing with NDs in optical fibers [5, 6]. Further optimization includes controlling the nanoparticle concentration (ultimately leading to single NV probes), improving the contrast by tuning laser and MW power, increasing sensitivity by using pulsed MW sequences, and design of the output grating and open-clad configuration for combining remote excitation and detection. Future applications can be found in magnetic field sensors, high resolution ultra-sensitive MRI imagers, and nanoscale NMR spectroscopy [7, 8].

References

[1] L. Rondin et al. "Magnetometry with nitrogen-vacancy defects in diamond", *Rep. Prog. Phys.* 77, 056503 (2014)

[2] S. L. Mouradian "Scalable integration of long-lived quantum memories into a photonic circuit" *Phys. Rev. X* 5, 031009, 2015.

[3] A. Z. Subramanian et al., "Low-loss singlemode PECVD SiN photonic wire waveguides for 532-900 nm wavelength window fabricated within a CMOS pilot line", *IEEE Photonics* 5(6), 2013.

[4] P. Neutens et al., "Development of a CMOS compatible biophotonics platform based on SiN nanophotonic waveguides", *Conference on Lasers and Electro-Optics (CLEO)* 10.1364/CLEO_AT.2014.JTh2A.31, 2014.

[5] X. Liu et al., "Fiber-integrated diamond-based magnetometer" *Appl. Phys. Lett.* 103, 143105, 2013.

[6] Y. Ruan et al. "Remote nanodiamond magnetometry" arXiv:1602.06611, 2016.

[7] D.R. Glenn et al., "Single-cell magnetic imaging using a quantum diamond microscope" *Nat. Methods* 12 (8) 736–738, 2015.

[8] F. Shi et al., "Single-protein spin resonance spectroscopy under ambient conditions", *Science* 347 (6226) 1135-1138, 2015.